Engineering Sciences

3D reconstruction size effect on the quantification of solid oxide fuel cell nickel-yttria-stabilized-zirconia anode microstructural information using scanning electron microscopy-focused ion beam technique

Zhenjun Jiao · Naoki Shikazono

Received: 26 January 2016/Revised: 1 March 2016/Accepted: 3 March 2016/Published online: 25 March 2016 © Science China Press and Springer-Verlag Berlin Heidelberg 2016

Abstract Self-made conventional nickel-yttria-stabilized zirconia composite anodes after reduction and 500 h operation were analyzed by three-dimensional microstructure reconstruction based on focused ion beam-scanning electron microscopy technique. Interfacial area, threephases-boundary density and phase volume fraction were measured based on the three-dimensional microstructure reconstruction to quantitatively study the statistical characterization of solid oxide fuel cell nickel-yttria-stabilizedzirconia anode microstructure before and after operation. It is found that for anode operated with long time, it is necessary to increase the corresponding three-dimensional reconstruction size to suppress the influence microstructure variation caused by Ni agglomeration in order to obtain more accurate microstructural quantification information.

Keywords FIB-SEM · 3D reconstruction · TPB density · Tetragonal mesh

1 Introduction

Solid oxide fuel cell (SOFC) has been treated as a high energy efficiency power generation system with fuel flexibility, which attracted more and more attentions in the last few decades. The usual operation temperature for SOFC anode made of nickel-yttria-stabilized zirconia (Ni-YSZ)

SPECIAL TOPIC: Modeling of Solid Oxide Fuel Cells

Z. Jiao (⊠) · N. Shikazono Institute of Industrial Science, The University of Tokyo, Tokyo 153-8505, Japan

e-mail: zhenjun@iis.u-tokyo.ac.jp

[1], ranged from 973 to 1273 K, results in the challenge of long time stability and durability of SOFC electrodes. The SOFC anode degradation mechanism has been intensively investigated, which is mainly caused by Ni coarsening, especially during the initial operation period [2–6]. Recently, three-dimensional (3D) reconstructions of SOFC electrode has been achieved by applying focused ion beamscanning electron microscopy (FIB-SEM) technique [6–11]. This technique provides quantitative information of composite cermet microstructure in 3D, which can be correlated to the electrode performance via specific surface areas and active three-phase boundary density [1]. Compared to quantitative characterization of composite cermet based on 2D images [5], FIB-SEM 3D reconstruction technique leads to more accurate microstructure analysis, and facilitates 3D electrochemical numerical simulation.

Several researchers have investigated the influence of 3D reconstruction size on the statistic quantitative information of composite cermet microstructure [12-15]. The maximum size of 3D reconstruction based on FIB-SEM technique was limited by SEM image drifting and shadow effects which is quite difficult to be solved in the current stage. The typical maximum length of FIB-SEM reconstruction is always under 30 µm, which might be insufficient to be used for extracting the representative quantitative information from a specific microstructure. In this paper, the effect of FIB-SEM 3D reconstruction size is quantitatively studied based on two 3D reconstructions with the largest sizes which we can supply with the current experimental conditions. Quantitative characterizations of microstructures of Ni-YSZ composite anodes after reduction and 500 h operation were compared to study the minimum size of 3D reconstruction which can be representative for the quantification of microstructural information.





2 Experimental

2.1 Anode fabrication and operation

Electrolyte-supported cells were used in this study. The anode cermet was prepared by ball-mixing NiO and YSZ powders (AGC Seimi Chem. Corp., Japan) for 48 h where the volume ratio of Ni-YSZ was 43 %:57 % after Ni reduction. The mixture was then mixed with terpineol solvent and the ethylcellulose binder in agate mortar to obtain anode slurry. The slurry was then screen-printed onto commercial dense 8 mol% YSZ pellet (diameter 20 mm, thickness 0.5 mm, Fine Ceramics Corp., Japan) with a diameter of 10 mm and then sintered at 1400 °C for 3 h. The cathode material was prepared by mixing (La_{0.8}Sr_{0.2})_{0.97}MnO₃ (LSM) powder with YSZ powder in a mass ratio of 50 %:50 %. Similar method as the anode was used to obtain cathode slurry. The slurry was screen-printed onto the counter side of the commercial YSZ pellet with a diameter of 10 mm as cathode. The cathode was then sintered at 1200 °C for 3 h. The anode was then operated in 3 % H₂O humidified hydrogen with a current density of 200 mA cm⁻² for 500 h to compare with the initial anode microstructure after reduction. The details of anode operation have been introduced in Ref. [6].

2.2 FIB-SEM observation

The anode samples before and after operation were observed by FIB-SEM (Carl Zeiss, NVision 40). The samples were first infiltrated by low viscosity epoxy resin under low pressure atmosphere (ca. 15 Pa). The samples were then polished by using Ar-ion beam cross-section polisher (JEOL Ltd., SM-09010) for FIB-SEM observation, so that the pores of the porous electrode could be distinguished during FIB-SEM observation as shown in Fig. 1. The white, gray and black regions correspond to Ni, YSZ and pore, respectively. The details of dual-beam FIB-SEM observation technique have been introduced in

Refs. [6, 11]. The 3D microstructure of the Ni-YSZ anodes before and after 500 h operation were virtually reconstructed based on 2D image series, as shown in Figs. 2

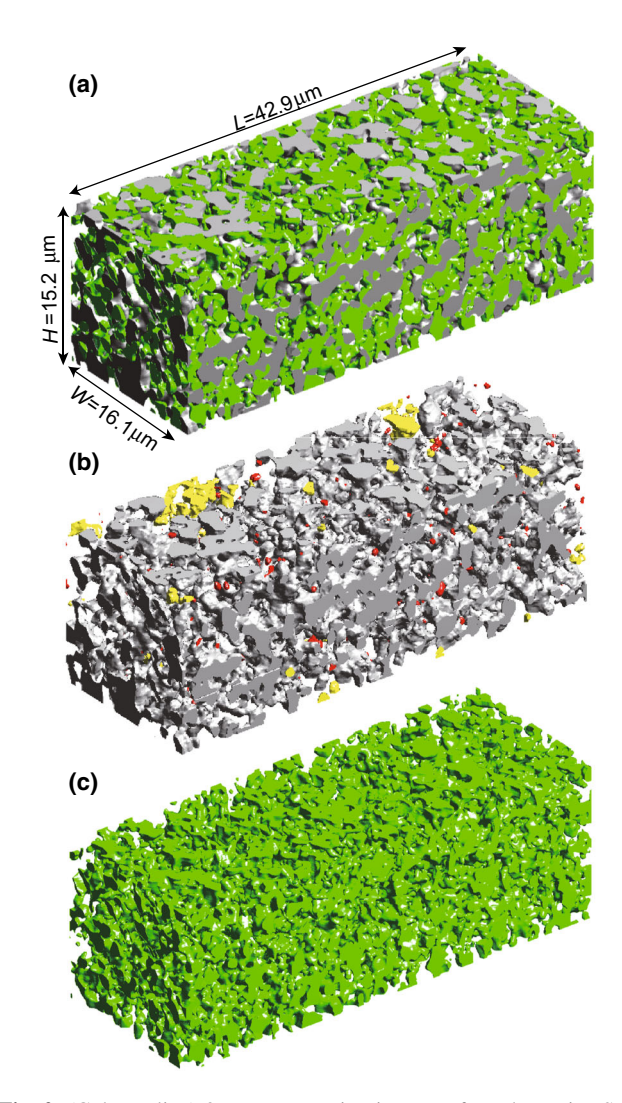


Fig. 2 (Color online) 3D reconstruction images of anode **a** Ni–YSZ, **b** Ni phase (red isolated particle, yellow unknown-status particle) and **c** YSZ phase after reduction. Gray Ni and green YSZ

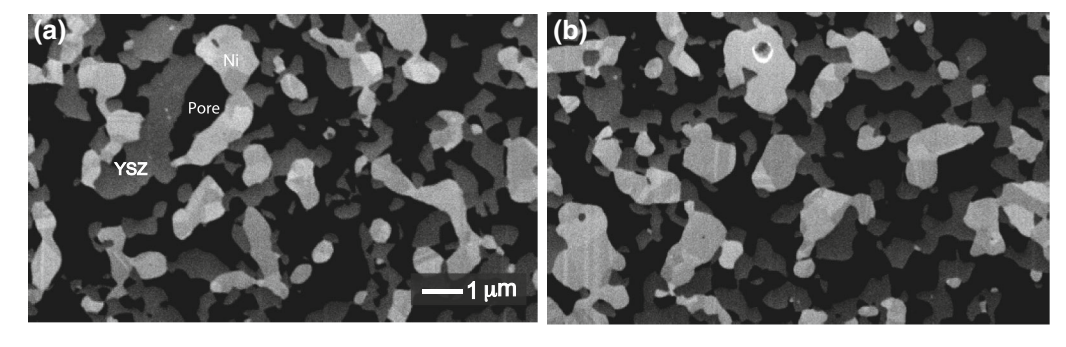


Fig. 1 2D SEM images of anodes (a) after reduction and (b) after 500 h operation. White Ni, gray YSZ and black pore





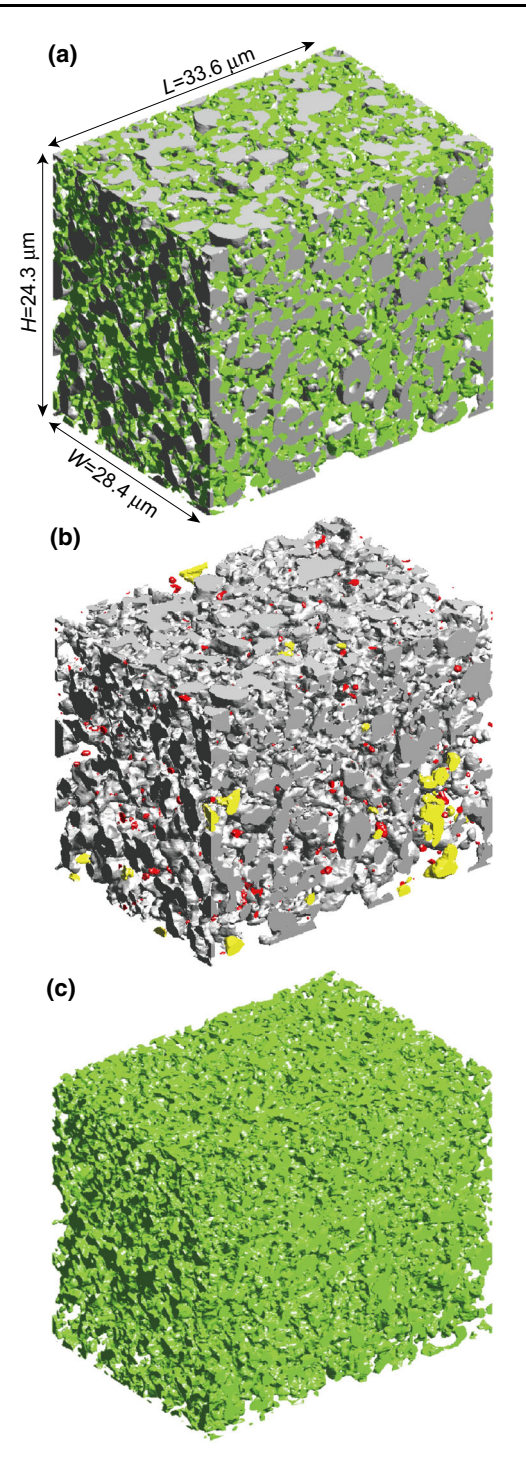


Fig. 3 (Color online) 3D reconstruction images of anode **a** Ni–YSZ, **b** Ni phase (red isolated particle, yellow unknown-status particle) and **c** YSZ phase after after 500 h operation with a current density of 0.2 A cm⁻². Gray: Ni and green YSZ

and 3. The Ni and YSZ phases are demonstrated as grey and green, respectively. In order to study the influence of size effect on 3D reconstruction quantification information, the 2D images were captured as large as possible during FIB-SEM polishing.

3 Results and discussion

The red particles in Figs. 2b and 3b indicate the isolated particles from the main network which connects to the six volumetric boundary faces. The yellow particles indicate the phase portion only connected to volumetric boundary faces with an unknown-status. It seems that the Ni phase percolation connectivity did not deteriorate obviously within operation time based on direct observation. It has been proven in Ref. [6] that YSZ can be treated as a stable phase without morphological change in the current operation environment. In order to quantify the microstructure change in operation, the phase volume fractions of percolated, isolated and unknown-status Ni phases were measured based on the 3D reconstructions and summarized in Table 1. TPB densities and surface areas were measured using tetragonal mesh method based on the 3D reconstructions by Matlab as shown in Fig. 4 [16].

In order to investigate the influence of FIB-SEM 3D reconstruction size on the quantification of anode microstructure, a new length factor x (0 < x < 1) was introduced. Nine sub-reconstructions were extracted at the center and along the eight conners of the original 3D reconstruction with the original width, length and height multiplied x. Figures 5 and 6 show three random Ni subreconstruction samples for x = 0.2, 0.4, 0.6 corresponding to Figs. 2b and 3b, respectively. It can be seen that for all the sub-reconstructions before and after operation, with x < 0.5, the percolation of Ni phase is very different from the original large-size reconstruction. It seems that the random microstructure variation is very large. For x > 0.5, the percolation of Ni phase becomes relatively stable compared to original large-size reconstruction for both cases. It is seen that reconstruction size can influence the result of percolation connectivity of Ni for both samples before and after operation.

Table 1 Volume fraction, and TPB density for anodes before and after 500 h operation

Sample	Percolated phase (%)	Isolated phase (%)	Unknown- status phase (%)
			Primate (70)
Ni before operation	97.81	0.64	1.55
YSZ before operation	98.49	0.67	0.84
Ni after 500 h operation	98.07	1.03	0.90
YSZ after 500 h operation	98.60	0.85	0.55





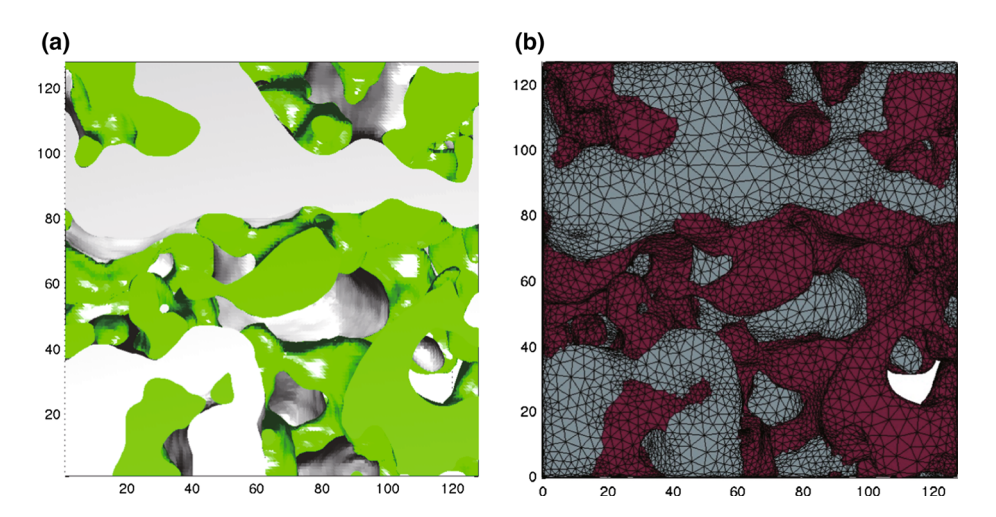


Fig. 4 (Color online) a A typical 3D reconstruction image of Ni–YSZ anode after reduction (gray Ni, green YSZ). b Corresponding tetragonal mesh generated based on the 3D reconstruction

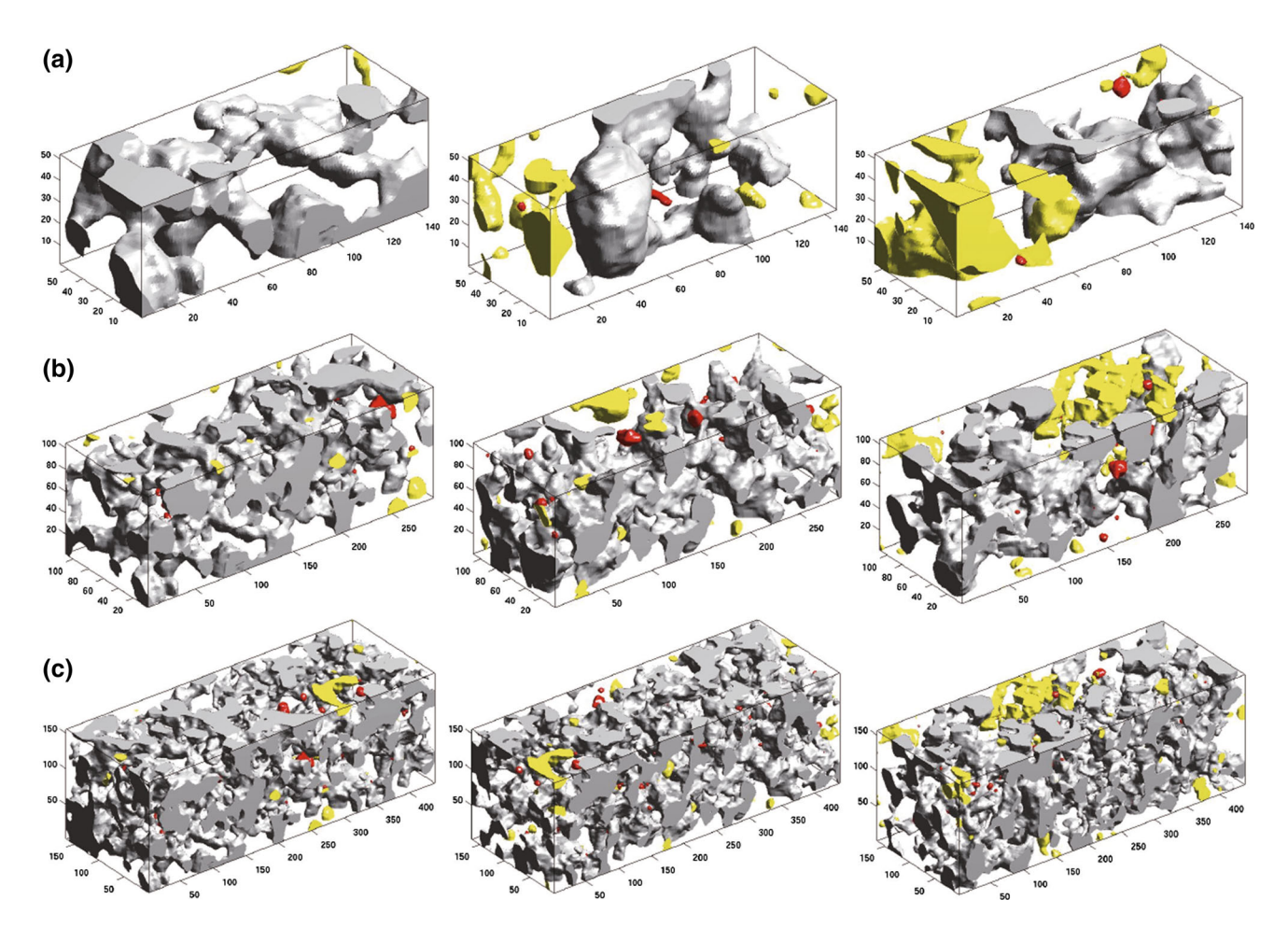


Fig. 5 (Color online) 3D reconstruction images of Ni sub-volumes with different x values, corresponding to Fig. 2b. Three randomly chosen reconstructions are shown for each x value. **a** x = 0.2, **b** x = 0.4 and **c** x = 0.6

In order to further quantify the microstructure variation, the specific interface areas, total and active TPB densities and phase volume fractions of Ni and YSZ measured base on all x dependent sub-reconstructions for samples before and after operation are compared as shown in Fig. 7. An allowed deviation of 15 % is chosen for all the parameters





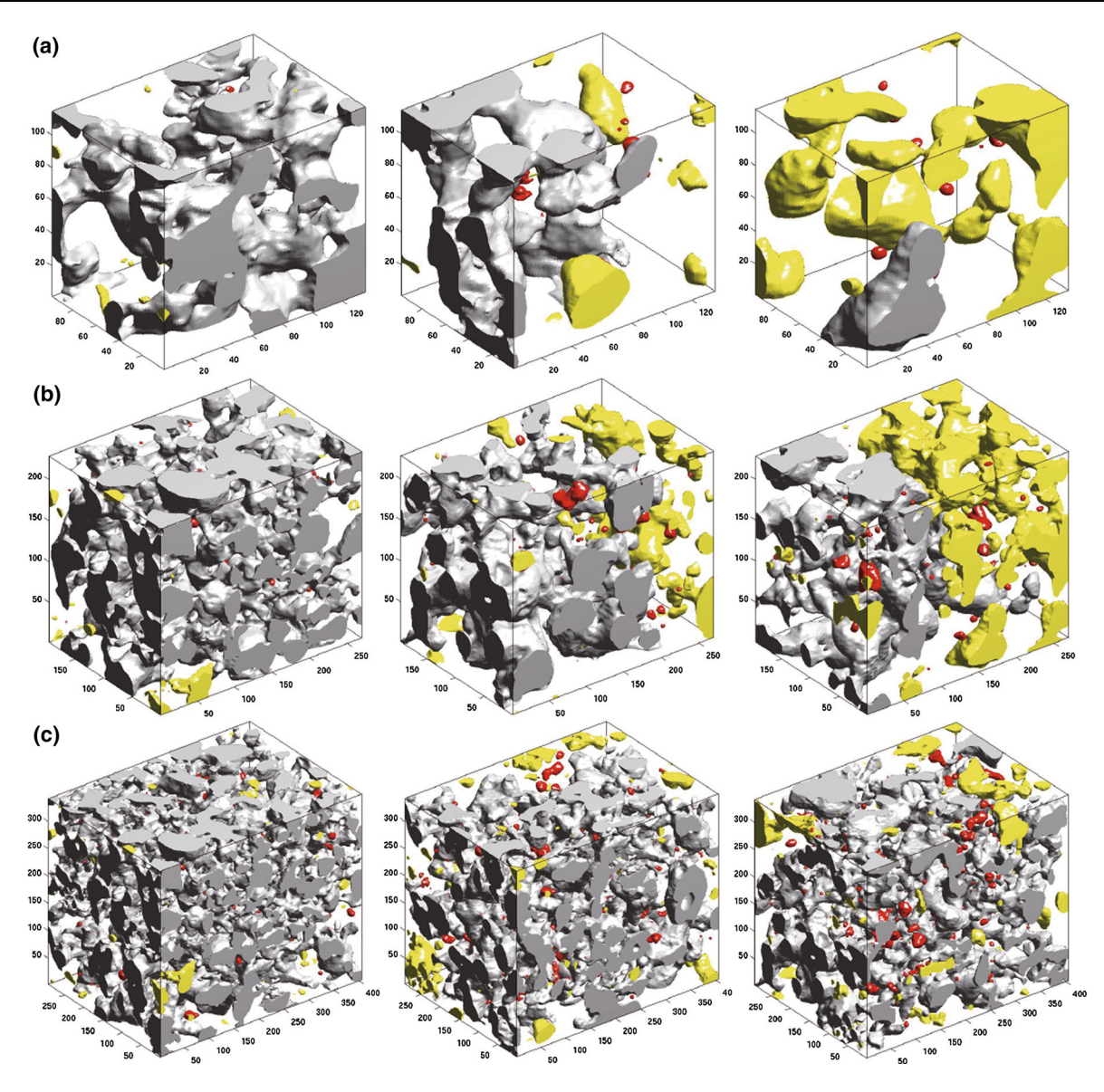


Fig. 6 (Color online) 3D reconstruction images of Ni sub-volumes with different x values, corresponding to Fig. 3b. Three randomly chosen reconstructions are shown for each x value. **a** x = 0.2, **b** x = 0.4 and **c** x = 0.6

in this study to be defined as stable status [14]. It is seen from Fig. 7a that the average specific Ni–YSZ, YSZ–Pore and Pore–Ni interfacial areas converge when x>0.4 with values of 0.5148, 1.0106 and 0.4685 μ m² μ m³ and very small error deviations of 0.0253, 0.0170 and 0.0098 μ m² μ m³, which can be neglected compared to allowed deviation. After 500 h operation, as shown in Fig. 7d, the average specific YSZ–Pore and Pore–Ni interfacial areas converge when x>0.4 with values of 1.0616 and 0.4330 μ m² μ m³ and larger error deviations of 0.0486 and 0.0251 μ m² μ m³ within the allowed deviation range. The average specific Ni–YSZ interfacial areas does not converge and the error deviation, about 30 %, is larger than 15 %, which makes the parameter considered to be unstable. Average specific YSZ–Pore interfacial area

increased a little after 500 h operation. It means that specific Ni surface area decreased in operation which can be attributed to the decrease of Ni free surface energy in sintering process. Figure 7b, e shows the average total and directional active TPB densities against x before and after 500 h operation. Directional active TPB density is defined as the TPB formed along a specific direction $(0 \rightarrow 1 \text{ or } 0 \leftarrow 1)$ in an axis, with Ni and YSZ phases connected to the faces of starting (0) and ending (1), respectively [8]. As shown in Fig. 7b, both average total and active TPB densities along different axes converge when x > 0.4 with a value of $1.9274 \,\mu\text{m}\,\mu\text{m}^{-3}$ and a small error deviation of $0.1059 \,\mu\text{m}\,\mu\text{m}^{-3}$, which can be accepted as stable status with a deviation of $5.5 \,\%$. After 500 h operation, as shown in Fig. 7e, both total and active average TPB densities





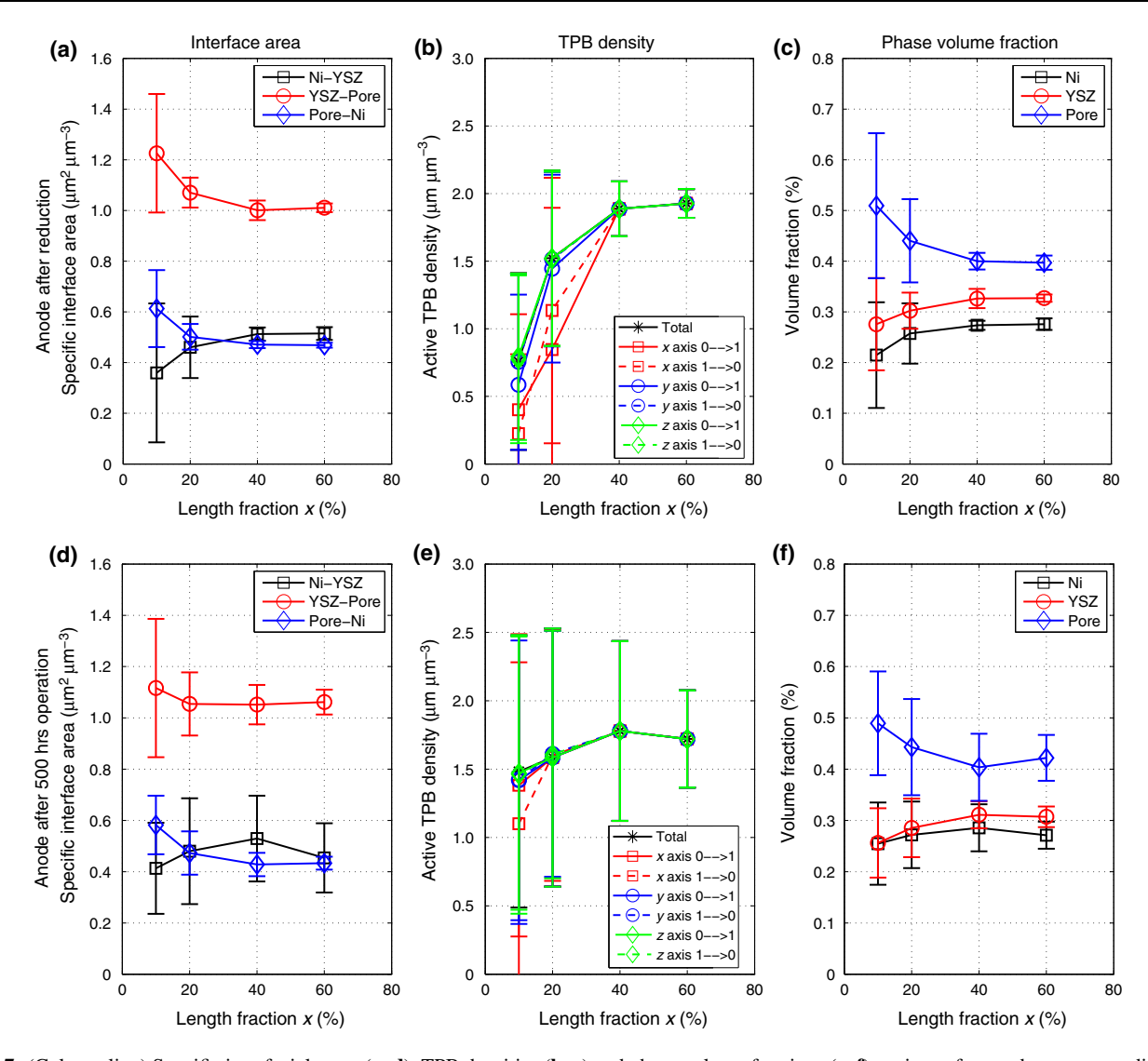


Fig. 7 (Color online) Specific interfacial areas (\mathbf{a}, \mathbf{d}) , TPB densities (\mathbf{b}, \mathbf{e}) and phase volume fractions (\mathbf{c}, \mathbf{f}) against x for anodes corresponding to Figs. 2a and 3a

along different axes do not fully converge when x > 0.4and the error deviation is about 20.7 %, which makes the parameter considered to be unstable. After 500 h operation, both average total and active TPB densities along different axes decreased to about $1.7203 \,\mu\mathrm{m}\,\mu\mathrm{m}^{-3}$. caused by Ni coarsening. In order to verify the composition percentages of different phases with different x, Fig. 7c, f shows the volume fractions of three phases before and after operation. It is shown in Fig. 7c that the average volume fraction of Ni, YSZ and pore phases converge when x > 0.4 with values of 27.58 %, 32.71 % and 39.71 % with small error deviations of 4.1 %, 2.2 % and 4.3 %, which can all be accepted as stable status. After 500 h operation, as shown in Fig. 7f, the average volume fraction of Ni, YSZ and pore phases do not fully converge when x > 0.4 and the error deviations are about 9.7 %, 6.5 % and 10.6 %, which increased by several times compared to the sample before operation. The volume fractions of three phases generally remain constant with slight changes compared to the results as shown in Fig. 7c.

Thus it can be concluded that the microstructure of anode before operation was relatively uniform and lost the uniformity after long time operation. Before the operation, an length factor of x > 0.4 is enough for quantifying the characterization of anode microstructure with a smaller FIB-SEM reconstruction size. After 500 h operation, The anode microstructure become non-uniform that even a larger FIB-SEM reconstruction size with an length factor x > 0.6 is insufficient for quantifying the characterization of anode microstructure. The microstructure randomness increased because of the agglomeration of Ni phase. An even larger 3D reconstruction size should be used for obtaining the relatively accurate quantification information of anode microstructure, which becomes a



challenge in the current stage. Most of the investigations based on FIB-SEM reconstructions with a relatively smaller size for anode after long-time operation should be modified based on this conclusion. It is necessary to increase the corresponding FIB-SEM 3D reconstruction size to suppress the influence of microstructure variation caused by Ni agglomeration in microstructural quantification to get more accurate microstructural information. Because of the limitation of computer capability, the quantifications of microstructures for both samples with x > 0.6 were not conducted. Based on the current results, it is seen that it is necessary to find the minimum 3D reconstruction size to quantify the morphological characterization of a sample when FIB-SEM reconstruction technique is used.

4 Conclusion

3D reconstructions based on FIB-SEM technique were used to quantify the self-made anode microstructure before and after 500 h operation with reconstruction sizes as large as possible. Specific interfacial area, TPB density and phase volume fraction were measured based on the 3D reconstruction to quantitatively study the statistical characterization of samples with a varying size controlled by a length factor x. It is found that the necessary 3D reconstruction size should increases with anode operation time in order to obtain the accurate microstructure quantification information. It is necessary to find the proper 3D reconstruction size, especially for the sample with long-time operation, to quantify the morphological characterization of a Ni-YSZ composite anode sample when FIB-SEM 3D reconstruction technique is used.

Acknowledgments This work was supported by the New Energy and Industrial Technology Development Organization (NEDO) under the Development of System and Elemental Technology on Solid Oxide Fuel Cell (SOFC) Project.

Conflicts of interest The authors declare that they have no conflict of interest.

References

 Subhash CS, Kevin K (2003) High temperature solid oxide fuel cells: fundamentals, design and applications. Elsevier, Amsterdam

- Holzer L, Munch B, Iwanschitz B et al (2011) Quantitative relationships between composition, particle size, triple phase boundary length and surface area in nickel-cermet anodes for solid oxide fuel cells. J Power Sources 196:7076–7089
- Chen HY, Yu HC, Cronin JS et al (2011) Simulation of coarsening in three-phase solid oxide fuel cell anodes. J Power Sources 196:1333–1337
- Badwal SPS, Bannister MJ, Hannink RHJ (2003) Science and technology of zirconia V. Technomic Publishing Company Inc, Melbourne, p 752
- Simwonis D, Tietz F, Stover D (2000) Nickel coarsening in annealed Ni/8YSZ anode substrates for solid oxide fuel cells. Solid State Ion 132:241–251
- Jiao ZJ, Shikazono N, Kasagi N (2012) Quantitative characterization of SOFC Nickel-YSZ anode microstructure degradation based on focused-ion-beam 3D-reconstruction technique. J Electrochem Soc 159:B285–B291
- Jiao ZJ, Lee G, Shikazono N et al (2012) Quantitative study on the correlation between solid oxide fuel cell Ni–YSZ composite anode performance and sintering temperature based on three-dimensional reconstruction. J Electrochem Soc 159:F278–F286
- Jiao ZJ, Shikazono N (2015) Quantitative study on the correlation between solid oxide fuel cell Ni–YSZ composite anode performance and reduction temperature based on three-dimensional reconstruction. J Electrochem Soc 162:F571–F578
- Sumi H, Kishida R, Kim JY et al (2009) Correlation between microstructural and electrochemical characteristics during redox cycles for Ni–YSZ anode of SOFCs. J Electrochem Soc 157:B1747–B1752
- Vivet N, Chupin S, Estrade E et al (2011) 3D microstructural characterization of a solid oxide fuel cell anode reconstructed by focused ion beam tomography. J Power Sources 196:7541–7549
- Iwai H, Shikazono N, Matsui T et al (2010) Quantification of SOFC anode microstructure based on dual beam FIB-SEM technique. J Power Sources 195:955–961
- Cai Q, Adjiman CS, Brandon NP (2009) Modelling the 3D microstructure and performance of solid oxide fuel cell electrodes: computational parameters. Electrochim Acta 56:5804– 5814
- 13. Rhazaoui K, Cai Q, Kishimoto M et al (2015) Towards the 3D modelling of the effective conductivity of solid oxide fuel cell electrodes—validation against experimental measurements and prediction of electrochemical performance. Electrochim Acta 168:139–147
- Zheng K, Zhang Y, Li L et al (2015) On the tortuosity factor of solid phase in solid oxide fuel cell electrodes. Int J Hydrog Energy 40:665–669
- Zheng K, Ni M (2016) Reconstruction of solid oxide fuel cell electrode microstructure and analysis of its effective conductivity. Sci Bull 61:78–85
- Fang Q, Boas D (2009) Tetrahedral mesh generation from volumetric binary and gray-scale images. In: Proceedings of IEEE international symposium on biomedical imaging—from nano to macro, vol 1–2, pp 1142–1145



